Contrib Mineral Petrol (2016) 171:102
DOI 10.1007/s00410-016-1315-z

ORIGINAL PAPER

Effect of temperature, pressure and iron content on the electrical conductivity of orthopyroxene

Baohua Zhang[1] · **Takashi Yoshino**[2]

Received: 5 September 2016 / Accepted: 4 November 2016 / Published online: 19 November 2016

Abstract The electrical conductivity of $(Mg_{1-x}, Fe_x)SiO_3$ orthopyroxene with various iron contents [X_{Fe} = Fe/(Fe + Mg) = 0, 0.1, 0.3, 0.5, 0.7 and 1.0] was measured in a Kawai-type multianvil apparatus by impedance spectroscopy over a wide range of pressure (P) and temperature (T) covering the stability field of orthopyroxene. Impedance spectroscopy measurements indicated that the electrical conductivity of orthopyroxene systematically increased with increasing total iron content. The conductivity slightly decreased with increasing pressure at a constant temperature. For samples with lower Fe content, two conduction mechanisms were identified from the Arrhenius behavior. A change in the activation enthalpy indicated that the dominant conduction mechanism changed from small polaron to ionic conduction with increasing temperature. At temperature below 1373 K, relatively low activation enthalpies and small positive activation volumes suggest that the dominant mechanism of charge transport is Fe^{2+}–Fe^{3+} hopping (small polaron). At higher temperatures above 1473 K, ionic conduction (via Mg vacancy mobility) dominates, with higher activation enthalpy exceeding 2 eV and larger positive activation volume. All electrical conductivity data fit the formula for electrical conductivity

$$\sigma = \sigma_0^i \exp\left[-\frac{(\Delta E_0^i + P\Delta V_0^i)}{k_B T}\right] + \sigma_0^p X_{Fe} \exp\left\{-\frac{\left[\Delta E_0^p - \alpha X_{Fe}^{1/3} + P(\Delta V_0^p - \beta X_{Fe})\right]}{k_B T}\right\},$$

where σ_0 is the pre-exponential term, ΔE_0 and ΔV_0 are the activation energy and the activation volume at very low total iron concentration, k_B is the Boltzmann constant, T is the absolute temperature, and superscripts i and p denote the ionic and small polaron conductions, respectively. Electrical conductivity of Al-free orthopyroxene with $X_{Fe} = 0.1$ is distinctly lower than that of olivine with $X_{Fe} = 0.1$. Above 3 GPa Al content in orthopyroxene becomes smaller in association with garnet formation. Unless iron content in orthopyroxene is considerably high ($X_{Fe} > 0.2$), orthopyroxene has little influence on the electrical structure of the upper mantle.

Keywords Electrical conductivity · Iron content · Orthopyroxene · Small polaron · Upper mantle

Introduction

Electrical conductivity is a physical parameter that can be obtained from electromagnetic surveys at the Earth's surface. A comparison of geophysical models with mineral properties would provide important constraints on mineralogy and composition of the Earth's mantle. Therefore, in situ laboratory measurements of the electrical conductivity of the major mantle phases under high-pressure and high-temperature and controlled thermodynamic conditions are very important for understanding the conductivity structure of the mantle.

Communicated by Hans Keppler.

✉ Baohua Zhang
zhangbaohua@vip.gyig.ac.cn

[1] Key Laboratory for High-Temperature and High-Pressure Study of the Earth's Interior, Institute of Geochemistry, Chinese Academy of Sciences, Guiyang 550081, Guizhou, China

[2] Institute for Planetary Materials, Okayama University, Misasa, Tottori-ken 682-0193, Japan

Orthopyroxene is the second most abundant constituent mineral of the shallow upper mantle, which constitutes about 20–40% of the minerals in the upper mantle (Ringwood 1975). Thus, electrical properties of orthopyroxene could have a considerable influence on the electrical conductivity structure of the upper mantle. However, the electrical conductivities of orthopyroxene have not been studied as thoroughly as olivine. Most previous measurements of the electrical conductivity of orthopyroxene considered only effects of chemical composition (Seifert et al. 1982; Xu and Shankland 1999) and water content (Dai and Karato 2009; Yang et al. 2012, Zhang et al. 2012). Electrical properties of iron-bearing minerals are highly sensitive to many factors such as temperature, pressure, oxygen fugacity (fO_2), Fe content, water (H_2O) content, electronic spin-state transitions. However, no systematic data have been reported on the conductivity of orthopyroxene as a function of temperature, pressure and Fe content.

The electrical conductivity is governed by the number of charge carriers and their mobility. The electrical conduction mechanism of the main iron-bearing mantle minerals has been considered to be hopping of small polarons associated with the charge transfer of electron holes between Fe^{2+} and Fe^{3+} (e.g., Poirier 1991; Hirsch et al. 1993; Xu et al. 2000; Romano et al. 2006; Yoshino and Katsura 2009). When $Fe^{3+}/\sum Fe$ is fixed, the conductivity of iron-bearing silicate minerals should be strongly controlled by the total Fe content (Yoshino et al. 2012). Little is known about the influence of Fe content on the electrical conductivity of orthopyroxene at high pressure.

Orthopyroxene has a wide pressure stability field until it transforms to high-pressure clinoenstatite above 8 GPa (Akashi et al. 2009). Thus, knowledge of the pressure dependence of the electrical conductivity of orthopyroxene is necessary to construct a reference conductivity-depth profile of the Earth's upper mantle. The pressure dependence of small polaron conduction in most ferromagnesian minerals is frequently characterized by a negative activation volume (ferropericlase: Dobson and Brodholt 2000; Ohta et al. 2007; Yoshino et al. 2012; bridgmanite: Goddat et al. 1999; Katsura et al. 2007; Sinmyo et al. 2014), because electron hole hopping is mainly controlled by a decrease in interatomic distance with pressure (e.g., Poirier 1991). However, many experimental studies on the pressure dependence of the electrical conductivity of olivine (e.g., Xu et al. 2000; Yoshino 2010; Yoshino et al. 2012) have not well constrained the activation volumes for electrical conduction in Fe-bearing olivine. For example, Yoshino et al. (2012) observed a negative activation volume (−0.29 to −0.67 cm^3/mol) for iron-rich olivine, whereas a positive one (0.09 to 1.48 cm^3/mol) was reported by Xu et al. (2000) and Dai et al. (2010) for iron-poor olivine. At present, there is no consensus on the pressure dependence of the electrical conductivity of upper mantle minerals.

In this study, we measure the electrical conductivity of anhydrous orthopyroxene with various iron contents ($X_{Fe} = 0$, 0.1, 0.3, 0.5, 0.7, 1.0) over a wide range of pressure (P) and temperature (T) covering the stability field of orthopyroxene. Such experimental investigations are crucial to understand the conduction mechanism and the origin of the mantle high conductivity layer, and also to provide some constraints on temperature, chemistry and the conductivity-depth profile in the Earth's upper mantle.

Experimental procedures

To investigate the effect of Fe contents on the electrical conductivity of orthopyroxene, we prepared starting materials with six different compositions of $(Mg_{1-x}, Fe_x)SiO_3$ with $x = 0$, 0.1, 0.3, 0.5, 0.7 and 1.0 from a mixture of MgO, Fe_2O_3 and SiO_2. The procedure is similar to our previous work (Zhang et al. 2012). The oxide powders were dried at 1273 K for 4 h, then mixed and ground in an agate mortar by hand. The glasses were synthesized from these mixtures by melting under ambient pressure at 1873 K in air and quenching them into water. These glasses were finely ground and pressed into pellets. The pellets were heated in an atmospheric-pressure furnace at 1473 K for a few hours using a CO_2 and H_2 gas mixture for controlled oxygen partial pressure close to the NNO buffer. The powder was loaded into a Ni capsule, and the Ni capsule inserted into a larger Pt tube with an outer diameter of 3.0 mm and wall thickness of 0.1 mm, the space between smaller Ni capsule and larger Pt capsule was filled by Ni and NiO powder mixture, and then sealed by welding. The samples ($X_{Fe} = 0.1$, 0.3, 0.5 and 0.7) were sintered in an end-loaded piston–cylinder apparatus at 1 GPa and various temperatures (900–1573 K) for several hours using 3/4″ in. pressure assemblies. A sintered sample with a diameter of 1.5 mm was cored from the center portion of the sintered orthopyroxene aggregate using an ultrasonic drilling machine. However, the enstatite ($X_{Fe} = 0$) sample was not pre-synthesized by piston–cylinder experiment but prepared from $MgSiO_3$ glass. A sample with ferrosilite composition ($X_{Fe} = 1.0$) was directly synthesized during the conductivity measurement run at high temperature, using mixtures of fayalite and silica as starting materials.

Before and after the conductivity measurements, phases in the recovered sample were confirmed to be orthopyroxene by micro-focus X-ray diffraction experiments. Also, recovered samples were doubly polished to ~100 μm thickness and measured by Fourier transformation infrared (FT-IR) spectroscopy using a Jasco FTIR-6200 instrument equipped with an IRT-7000 infrared microscope, at

50 × 50 μm aperture size large enough to incorporate dozens of grains. At least five different spots were measured for each sample using unpolarized light. Paterson's calibration (Paterson 1982) was adopted to calculate the water content, with an integration range of 2600–4000 cm^{-1}. The representative IR spectra of orthopyroxene aggregates before and after the electrical conductivity measurement are shown in Fig. 1. In this study, FT-IR spectra indicate that the samples are almost dry (<3 wt.ppm) during the whole experimental process. Thus, proton conduction would be ruled out as the dominant conduction mechanism.

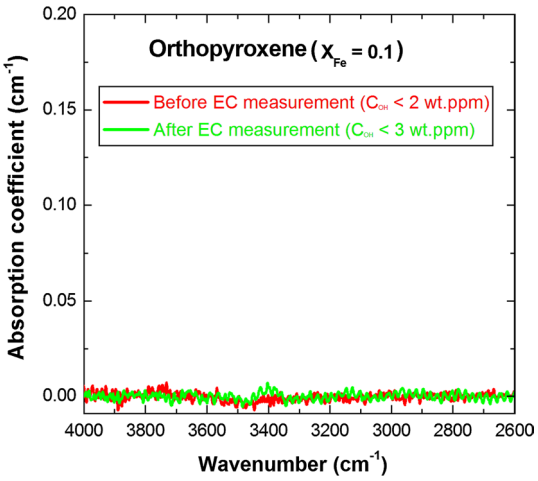

Fig. 1 Unpolarized FT-IR spectra of orthopyroxene aggregates before ($X_{Fe} = 0.1$) and after (5K2888) the conductivity measurements

The electrical conductivity measurements were conducted in a Kawai-type multianvil apparatus installed at the Institute for Planetary Materials, Okayama University. The cell assembly is essentially the same as that in our previous studies (Yoshino et al. 2006). The pressure was calibrated at high temperature by the phase transition of albite to jadeite (900 °C and 2.4 GPa) (Holland 1980) and by the conductivity jump due to the phase transition ($\alpha \rightarrow \gamma$) for fayalite (1100 °C and 5.6 GPa, 1300 °C and 6.6 GPa) (Akimoto et al. 1967; Yoshino et al. 2012). Oxygen fugacity (fO_2) is an important factor affecting the electrical conductivity of minerals that contain variable valence elements (especially Fe). In the present conductivity measurements, a sample was sandwiched by two Ni electrodes to maintain an oxygen fugacity close to the Ni–NiO buffer. Before conductivity measurement, Ni electrodes were baked in the air at 1273 K for 4 h to form a thin oxide layer, and then, the upper and lower surfaces which touch the sample were polished to remove the NiO layer. This method is same as in a previous study in our group (Guo et al. 2011).

Electrical conductivity measurements were performed at three different loads (1.5, 3.5 and 5 GPa) using a Solartron 1260 Impedance/Gain-Phase Analyzer (combined with a Solartron 1296 interface if the sample resistance was higher than MΩ) at conditions of T = 573–1773 K (Table 1). The complex impedance spectra were obtained

Table 1 Summary of experimental results

Run no.	Sample (X_{Fe})	P (GPa)	T (K)	Oxygen buffer	σ_0 (S/m)	ΔE (eV)	ΔV (cm^3/mol)
5K2893	0	1.5–5	1173–1773	NNO	$10^{5.53}$ (245)	2.46 ± 0.11	1.84 ± 0.80
5K2888	0.1	1.5–5	773–1673	NNO	668 (184)	1.59 ± 0.06	1.19 ± 0.70
	0.1	1.5–5	773–1373	NNO	73 (3)†	1.44 ± 0.06†	1.35 ± 0.45†
	0.1	1.5–5	1423–1673	NNO	$10^{7.46}$ (37)‡	2.99 ± 0.18‡	3.88 ± 0.51‡
5K2878	0.3	1.5–5	573–1673	NNO	28 (2)	0.94 ± 0.04	1.31 ± 0.57
	0.3	1.5–5	573–1273	NNO	4 (2)†	0.84 ± 0.03†	0.65 ± 0.41†
	0.3	1.5–5	1373–1673	NNO	$10^{4.55}$ (5)‡	1.65 ± 0.21‡	2.39 ± 0.82‡
5K2885	0.5	1.5–5	573–1373	NNO	118 (11)	0.79 ± 0.01	0.28 ± 0.09
5K2884	0.5	1.5	673–1373	NNO	71 (12)	0.71 ± 0.01	
5K2890	0.7	1.5–5	473–1373	NNO	270 (11)	0.62 ± 0.05	0.95 ± 0.08
	0.7	1.5–5	473–1373	NNO	$10^{5.78}$ (1)§	0.68 ± 0.01§	0.95 ± 0.06§
5K2896	1.0	3.5–5	1173–1673	NNO	691 (118)	0.51 ± 0.02	1.52 ± 0.20
XS98[a]	0.08	5	1273–1673	MMO	5248	1.80 ± 0.02	
DK09[b]	0.14–0.18	8	873–1473	MMO	531 (15)	1.52 ± 0.06	

All data were fitted by Eq. (3) in this study

Numbers in parentheses are the errors by the nonlinear least squares fitting (1 sigma stand deviation)

† and ‡ represent the present data for low- and high-temperature regimes are separately fitted by Eq. (3), respectively

§ All data were fitted by Eq. (4)

[a] Xu and Shankland (1999)

[b] Dai and Karato (2009)

at 1.0-V amplitude and at frequencies ranging from 10^6 to 10^{-1} Hz. The samples were compressed in a stepwise fashion with a press load, heated to the desired temperature (573–1773 K) and then cooled to the lowest temperature at which measuring well-defined impedance spectra was possible. The temperature was changed in 50 or 100 K steps, and the electrical conductivity was measured at each temperature step. Sample conductivity (σ) was calculated from the sample resistance R (Ω), sample thickness L (m) and cross-sectional area of sample S (m^2) after conductivity measurements by means of the relation $\sigma = L/(R \times S)$. During compression and heating, the change in the sample dimension (L/S) was less than 5%.

Results

Recovered samples after the conductivity measurement were confirmed to be orthopyroxene by a micro-focus X-ray diffractometer in reflection geometry. The average grain size of orthopyroxene aggregates is around 10 μm. Figure 2 shows examples of impedance spectra acquired for $(Mg_{1-x}, Fe_x)SiO_3$ orthopyroxene samples under 5 GPa and different temperatures. For the low resistance sample (<1000 Ω), the shape of the spectrum shows the inductance part derived from the electrode at the high-frequency region at positive Z''. For high resistance samples (low X_{Fe}), the shape of the impedance arcs in the complex plane (Fig. 2) is a semi-circle, with the center located near the real axis Z', justifying the use of a simple RC parallel equivalent circuit to determine the sample resistance.

The temperature dependence of conductivity (σ) can be expressed according to the Arrhenius relation:

$$\sigma = \sigma_0 \exp\left(-\frac{\Delta H}{k_B T}\right), \tag{1}$$

where σ_0 is the pre-exponential factor, ΔH is the activation enthalpy (eV), k_B is the Boltzmann constant, and T is the absolute temperature. If the pressure effect on the conductivity is considered, the activation enthalpy (ΔH) is defined as

$$\Delta H = \Delta E + P\Delta V \tag{2}$$

where ΔE is the activation energy and ΔV is the activation volume. Consequently, Eq. (1) can be rewritten as

$$\sigma = \sigma_0 \exp\left(-\frac{\Delta E + P\Delta V}{k_B T}\right), \tag{3}$$

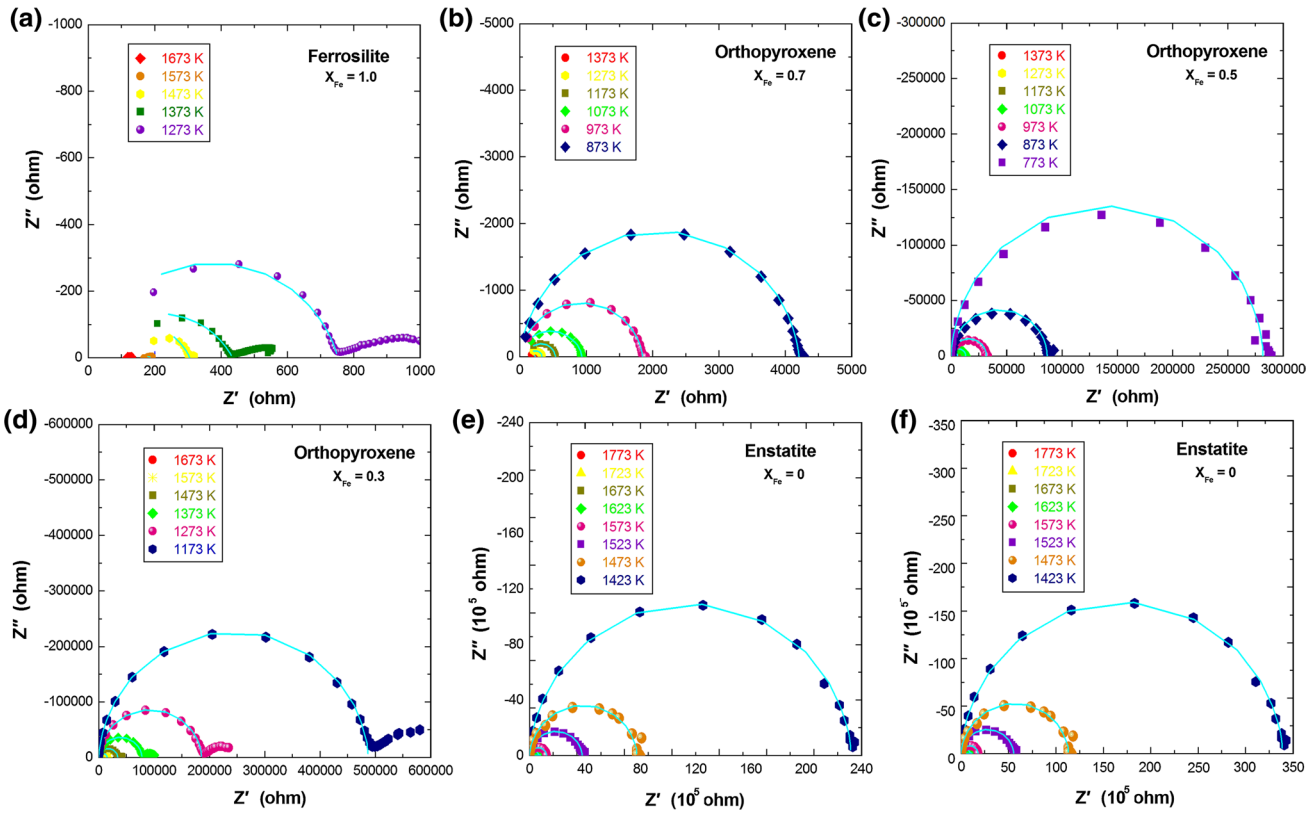

Fig. 2 Complex impedance spectra for $(Mg_{1-x}, Fe_x)SiO_3$ orthopyroxene aggregates with various X_{Fe} at frequencies ranging from 1 MHz to 0.1 Hz at the temperatures indicated

The pre-exponential factor, the activation energy (ΔE) and the activation volume (ΔV) for each sample are summarized in Table 1. Figure 3 shows the electrical conductivity obtained for orthopyroxene with various iron content at various temperatures as a function of pressure. The electrical conductivities of all samples decreased with increasing pressure at constant temperatures in the stability field of orthopyroxene. This trend suggests that the activation volume (ΔV) is positive. For ferrosilite ($X_{Fe} = 1.0$) (Fig. 3f), the conductivity was measured at higher temperatures (>1173 K) and pressures (3.5 and 5 GPa) because of the instability of ferrosilite (Akimoto et al. 1965).

Figure 4 shows the effect of temperature on the electrical conductivity of orthopyroxene ($X_{Fe} = 0$, 0.1, 0.3, 0.5, 0.7 and 1.0) as obtained at the highest pressure within stability field of orthopyroxene in an Arrhenius plot. The electrical conductivity of orthopyroxene aggregates

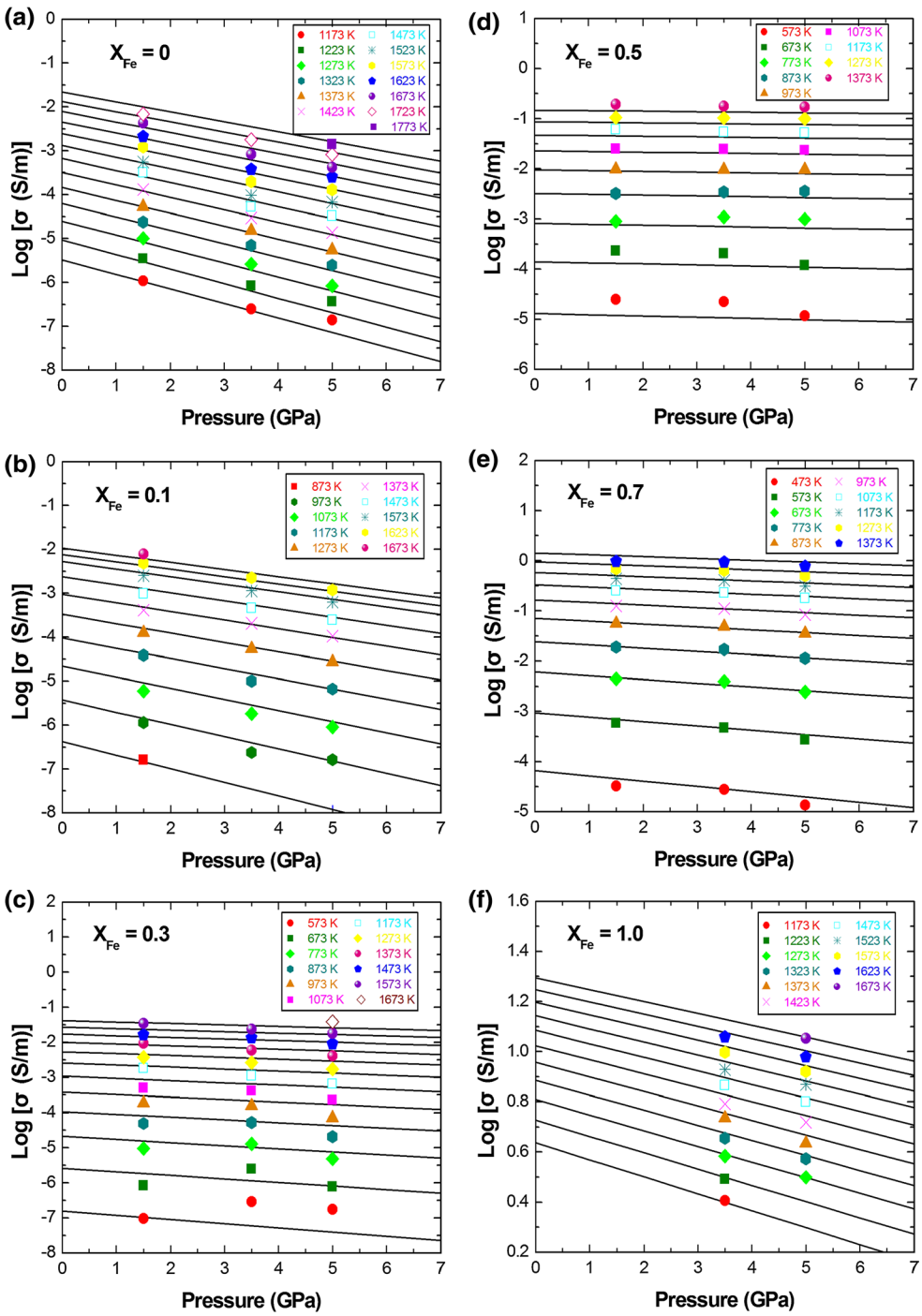

Fig. 3 Electrical conductivity of $(Mg_{1-x}, Fe_x)SiO_3$ orthopyroxene as a function of pressure at variable temperatures. **a** $X_{Fe} = 0$. **b** $X_{Fe} = 0.1$. **c** $X_{Fe} = 0.3$. **d** $X_{Fe} = 0.5$. **e** $X_{Fe} = 0.7$. **f** $X_{Fe} = 1.0$. In general, the conductivity of orthopyroxene decreases with increasing pressure at constant temperature. *Solid lines* indicate the electrical conductivity calculated by data fitting from Eq. (3) as a function of temperature and pressure. The fitted parameters in Table 1 were used for this calculation

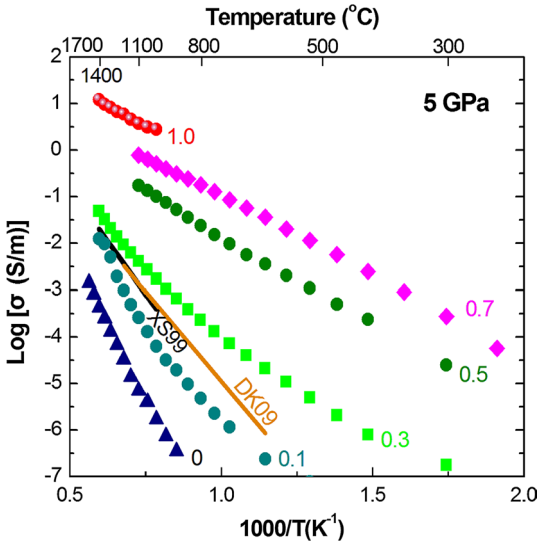

Fig. 4 Electrical conductivities of $(Mg_{1-x}, Fe_x)SiO_3$ orthopyroxene plotted as a function of reciprocal temperature at the highest pressure (5 GPa) in the stability field. Legend indicates sample compositions, given as X_{Fe}. *Solid lines* represent the Arrhenius plot of the electrical conductivities of orthopyroxene measured at 5 GPa (Xu and Shankland 1999) and 8 GPa (Dai and Karato 2009), respectively. Note that the electrical conductivity increases with total iron content in orthopyroxene aggregates. The slops in Arrhenius plot become steeper with decreasing iron content

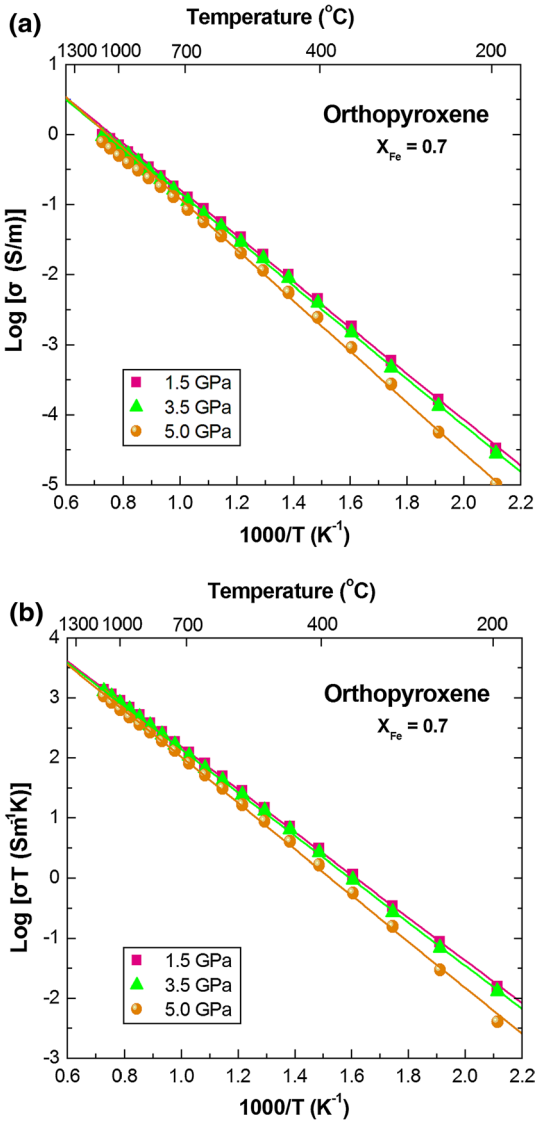

Fig. 5 Electrical conductivity variation as a function of reciprocal temperature for a Mg# of 30 orthopyroxene (5K2890) under different pressures. **a** Electrical conductivity versus reciprocal temperature. Note that the conductivity data follow an upward concave curve; *solid straight lines* are provided as a reference. **b** Electrical conductivity times temperature versus reciprocal temperature. The *solid lines* indicate the fitting results corresponding to Eq. (4)

increases with increasing total iron content. As shown in Fig. 3, variations of conductivity values and activation enthalpy as a function of pressure and temperature reproduced from Eq. (3) can explain the present results very well. However, two notable features can be found in Fig. 4. One is that the electrical conductivity data for orthopyroxene samples with low iron content ($X_{Fe} = 0$, 0.1, 0.3) show a kink in the Arrhenius plot. Another finding is that the electrical conductivity versus reciprocal temperature for the orthopyroxene sample with higher iron content ($X_{Fe} = 0.7$) shows an upward concave curve (Fig. 4). This behavior is similar to those of Al-bearing bridgmanite reported by Xu and McCammon (2002) and Yoshino et al. (2016). As illustrated in Fig. 5a, the relationship between log σ and the reciprocal temperature ($1/T$) cannot be fitted using a straight line as described by Eq. (1). On the contrary, such conductivity data can be fitted well by the following equation:

$$\sigma = \frac{\sigma_0}{T} \exp\left(-\frac{\Delta H}{k_B T}\right), \tag{4}$$

Figure 5b shows a perfect fit for orthopyroxene with $X_{Fe} = 0.7$ in the plot of $\log(\sigma T)$ vs $1000/T$ by Eq. (4).

Discussion

Effect of iron content on the electrical conductivity

Figure 6 shows the electrical conductivity as a function of iron content (X_{Fe}) at 1273 K for orthopyroxene measured at 5 GPa (this study) together with results of synthetic polycrystalline olivine (Hinze et al. 1981; Hirsch et al. 1993; Yoshino et al. 2009), synthetic polycrystalline garnet at 10 GPa (Romano et al. 2006) and synthetic

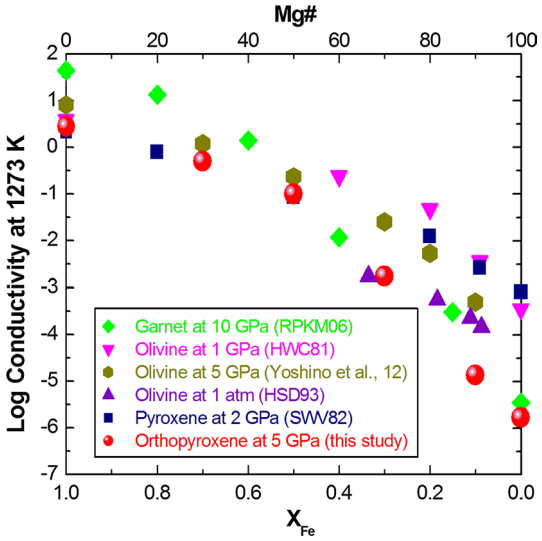

Fig. 6 Electrical conductivities of $(Mg_{1-x}, Fe_x)SiO_3$ orthopyroxene at 1273 K plotted as a function of composition X_{Fe}. Also shown are data for garnet (*diamonds*) taken from Romano et al. (2006), synthetic olivine at 1 GPa (*inverted triangles*), 5 GPa (*hexagons*) and 1 atm (*triangles*) taken from Hinze et al. (1981), Yoshino et al. (2012) and Hirsch et al. (1993), respectively, and synthetic pyroxenes (*squares*) taken from Seifert et al. (1982) at the same temperature

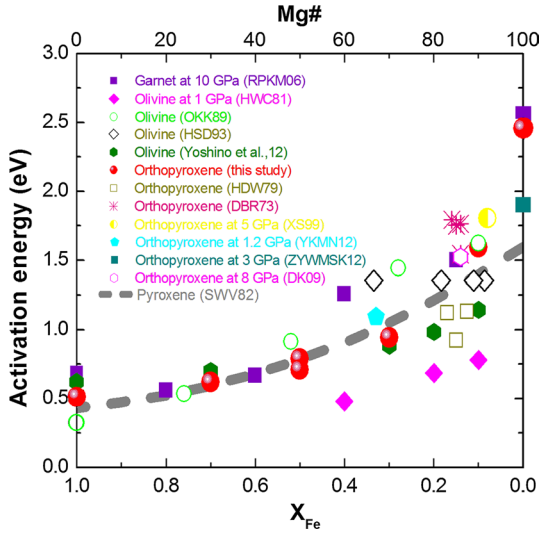

Fig. 7 Activation energies for the electrical conductivity in $(Mg_{1-x}, Fe_x)SiO_3$ orthopyroxene plotted as a function of composition X_{Fe}. *Data source*: RPKM06 (Romano et al. 2006); HWC81 (Hinze et al. 1981); HSD93 (Hirsch et al. 1993); OKK89 (Omura et al. 1989); HDW79 (Huebner et al. 1979); DBR73 (Duba et al. 1973); XS99 (Xu and Shankland 1999); YKMN12 (Yang et al. 2012); ZYWMSK12 (Zhang et al. 2012); DK09 (Dai and Karato 2009). *Dashed gray line* [SWV82] indicates activation enthalpies for pyroxenes taken from Seifert et al. (1982)

polycrystalline pyroxene at 2 GPa (Seifert et al. 1982). Each data set displays a strong positive dependence of the electrical conductivity on changing iron content, and the absolute conductivity values increase with increasing total Fe content under the same oxygen buffer (Hinze et al. 1981; Seifert et al. 1982; Romano et al. 2006; Yoshino and Katsura 2009; Yoshino et al. 2011, 2012). The conductivity of iron-bearing silicate minerals, especially for hopping conduction, should be strongly controlled by the total Fe content and $Fe^{3+}/\Sigma Fe$ ratio (Xu and McCammon 2002; Yoshino and Katsura 2009; Yoshino et al. 2016). Previous experimental investigations have demonstrated that incorporation of Al in some ferromagnesian minerals (specifically for orthoenstatite and bridgmanite) could help to stabilize Fe^{3+} in the crystal structure and may increase its Fe^{3+} concentration (Xu and Shankland 1999; Xu and McCammon 2002; Yoshino et al. 2016). At the same oxygen buffer condition, the Fe^{3+} concentration in the Al-free system is very small and much lower than that in the Al-bearing system. However, even small amounts of Fe^{3+} can also control its electrical conductivity (Xu and Shankland 1999; Xu and McCammon 2002; Yoshino et al. 2016). Thus, the electrical conductivity of Al-free orthopyroxene strongly depends on the total iron content.

In order to clarify the effect of Al content on the electrical conductivity of orthopyroxene, Fig. 4 shows a comparison of present results on Al-free orthopyroxene with some previous studies on Al-bearing systems. Xu and Shankland (1999) reported the electrical conductivity of $Mg_{0.92}Fe_{0.08}SiO_3$ orthopyroxene with 2.89 wt% Al_2O_3 at 5 GPa and at high temperatures ranging from 1273 to 1673 K. Dai and Karato (2009) measured the electrical conductivity of single-crystal orthoenstatite with 0.4–0.8 wt% Al_2O_3 at 8 GPa and temperature up to 1473 K. It is worth noting that although a relatively reduced oxygen fugacity buffer (M_O–MoO_2) was employed in Xu's and Dai's experiments as compared to the Ni–NiO buffer in this study, both previously reported conductivity values are slightly higher than that of the present result on orthopyroxene with $X_{Fe} = 0.1$ (Fig. 4). This discrepancy is mainly due to their samples containing significant Al. As discussed above, incorporation of Al in orthopyroxene could help to stabilize Fe^{3+} in the crystal structure and increase its Fe^{3+} concentration (Xu and Shankland 1999). Thus, the electrical conductivity of Al-bearing orthopyroxene could be significantly enhanced by small amounts of Fe^{3+} due to incorporation of Al in the orthopyroxene crystal structure, even when the iron content is relatively low or the oxygen fugacity buffer is relatively reduced.

Figure 7 shows activation enthalpies for the electrical conductivity of orthopyroxene plotted as a function of total Fe content (X_{Fe}). The activation enthalpy decreases from 2.46 to 0.51 eV with increasing X_{Fe} from 0 to 1.0. The variation of activation enthalpies of orthopyroxene is

quite similar to those of olivine along the forsterite–fayalite join (Omura et al. 1989; Yoshino et al. 2012), of orthopyroxene along the ferrosilite–enstatite (Seifert et al. 1982) and of garnet along the almandine–pyrope join at 10 GPa (Romano et al. 2006). Remarkably, Hirsch et al. (1993) reported the electrical conductivity of synthetic polycrystalline olivine with X_{Fe} ranging from 0.087 to 0.335 at atmospheric pressure. However, their results show no clear dependence of activation enthalpy on iron content (Fig. 7) because the very narrow temperature range in Hirsch et al.'s experiment might have prevented a reliable determination of activation enthalpies.

Charge transport mechanisms in orthopyroxene

Electronic conduction in silicate minerals is thermally activated with energy barriers for formation and migration of charge carriers. Possible electron conduction mechanisms for the constituent mantle minerals include ionic (vacancy), proton (H^+) and small polaron conductions. Ionic conduction can occur at higher temperatures through the creation of cation vacancies. Its charge carrier is generally considered to be vacancies in the magnesium site (V''_{Mg}). As a consequence, quite high activation enthalpies (>2 eV) and large positive activation volumes (several cm^3/mol) may result from an intrinsic mechanism such as ionic conduction at high temperatures (Schock et al. 1989; Yoshino et al. 2009; Yoshino 2010). Proton conduction is the other dominant conduction mechanism in nominally anhydrous minerals (NAMs) at low temperatures. However, proton conduction is unlikely to be a main conduction mechanism because our orthopyroxene samples contain no significant amount of water (Fig. 1).

In the ferromagnesian mantle minerals, a small polaron has been considered as a dominant charge carrier in which charge transfers occur by electron–hole hopping between ferric and ferrous ions (Hirsch et al. 1993; Xu et al. 2000; Romano et al. 2006; Yoshino and Katsura 2009; Yoshino et al. 2009, 2012):

$$Fe^{X}_{Me} + \dot{h} = Fe^{\bullet}_{Me} \quad (5)$$

As illustrated in Fig. 4, the conductivity data show a curve in the Arrhenius plot for orthopyroxene samples with low iron content ($X_{Fe} = 0$, 0.1 and 0.3). Such curvature represents a change from electron hole hopping mechanism (small polaron) to another conduction mechanism more favorable at high temperatures, such as Mg vacancy mobility. A change in conduction mechanism for olivine (Fo_{90}) from small polaron to ionic conduction has been proposed by Schock et al. (1989) at around 1600 K and at atmospheric pressure and by Yoshino et al. (2009) at around 1700 K and at 10 GPa. As X_{Fe} increases, conductivity values increase, while activation enthalpy decreases (Fig. 4; Table 1). Below 1373 K, the activation energies determined from each sample by Eq. (3) ranged from 0.51 to 1.59 eV. These values are comparable to those for the small polaron conduction of olivine (0.61–1.47 eV: Xu et al. 2000; Yoshino et al. 2012), wadsleyite (0.84–1.49 eV: Yoshino et al. 2012), ringwoodite (0.19–1.44 eV: Yoshino and Katsura 2009; Yoshino et al. 2012) and garnet (0.57–1.50 eV: Romano et al. 2006), suggesting that a small polaron is the dominant charge transport mechanism in orthopyroxene at low-temperature regimes.

Unlike for olivine, few studies have investigated the effect of pressure on the electrical conductivity of orthopyroxene. In general, pressure has been thought to have a small influence on the electrical properties of minerals (e.g., Xu et al. 2000). The present study demonstrated the negative effect of pressure on the electrical conductivity of orthopyroxene (Fig. 3). This observation suggests that the electrical conduction in orthopyroxene is characterized by a positive activation volume (see Table 1; Fig. 8). In fact, most of the previous conductivity measurements for small polaron conduction in silicate minerals as a function of pressure have revealed a small negative activation volume, including bridgmanite (Shankland et al. 1993; Katsura et al. 2007), ferropericlase (Yoshino et al. 2011), ilmenite (Katsura et al. 2007), olivine and its high-pressure polymorphs (Yoshino et al. 2012). For bridgmanite, Shankland et al. (1993)

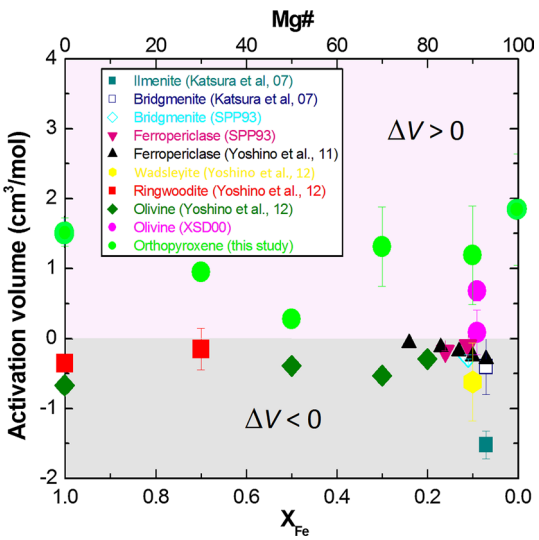

Fig. 8 Activation volume versus total iron content for small polaron conduction of major mantle minerals. Note that the activation volumes determined by this study are located in a positive field. *Data source*: Ilmenite (Katsura et al. 2007); Bridgmanite (Shankland et al. 1993; Katsura et al. 2007); Ferropericlase (Shankland et al. 1993; Yoshino et al. 2011); Ringwoodite (Yoshino et al. 2012); Wadsleyite (Yoshino et al. 2012); Olivine (Xu et al. 2000; Yoshino et al. 2012)

and Katsura et al. (2007) reported a small negative activation volume of −0.1 to −0.4 cm^3/mol. For ferropericlase, Yoshino et al. (2011) reported that the activation volume decreases from −0.07 to −0.20 cm^3/mol with X_{Fe} decreasing from 0.24 to 0.07. Recently, a small negative activation volume (−0.15 to −0.67 cm^3/mol) was also reported by Yoshino et al. (2012) for small polaron conduction in olivine and its high-pressure polymorphs (i.e., wadsleyite and ringwoodite). However, for olivine with low X_{Fe}, a positive activation volume has been reported based on conductivity measurements over a relatively wide pressure range (12.72 cm^3/mol: Omura et al. 1989; 0.09 to 1.48 cm^3/mol: Xu et al. 2000). In this study, the activation volumes calculated from the orthopyroxene samples with various X_{Fe} are always positive and larger than 2 cm^3/mol for the orthopyroxene with lower X_{Fe}, suggesting that ionic conduction is dominant in the higher-temperature regimes. In contrast, a small positive activation volume is consistent with small polaron conduction in the lower-temperature range (Xu et al. 2000). In all previous works, the small negative activation volume for small polaron conduction in silicates has been attributed to a decrease in the average Fe^{3+}–Fe^{2+} distance with increasing pressure that finally enhances conductivity (e.g., Shankland et al. 1993; Romano et al. 2006; Katsura et al. 2007; Yoshino et al. 2011, 2012), whereas the positive sign of activation volume has been attributed to the result of increased lattice deformation as a function of pressure (Xu et al. 2000). The positive activation volume for the conduction in orthopyroxene at lower temperatures could indicate considerable lattice shrinkage induced by a presence of Fe^{3+} in the octahedral site due to pressurization (Nestola et al. 2008).

At higher temperatures (>1373 K), the activation energy (1.65–2.99 eV) and the pre-exponential factor determined from the samples with low iron content ($X_{Fe} = 0$, 0.1 and 0.3) were much higher than those of the small polaron conduction in the low-temperature ranges (Table 1). Moreover, unlike the small polaron conduction showing a strong dependence of Fe content on the electrical conductivity and activation enthalpy (Omura et al. 1989; Romano et al. 2006; Yoshino et al. 2011, 2012), the present results show that the electrical conductivity of orthopyroxene samples with low X_{Fe} is insensitive to Fe content at temperature above 1373 K (Fig. 4). These observations suggest that ionic conduction could be the dominant charge transport mechanism for orthopyroxene at higher temperature. It is worth noting that ionic conduction in bridgmanite has been confirmed to be caused by the migration of extrinsic oxygen vacancies related to impurities such as Na^+, Al^{3+} and Fe^{3+} in bridgmanite (Xu and McCammon 2002; Dobson 2003; Yoshino et al. 2016). However, the activation enthalpies derived from oxygen ionic conduction in bridgmanite (1.47 eV: Xu and McCammon 2002; 1.42 eV: Dobson 2003; 0.79–1.17 eV: Yoshino et al. 2016) are much lower than those observed in orthopyroxene (2.46–2.99 eV: this study) and in olivine (2.14–2.25 eV: Yoshino et al. 2009). Note that the self-diffusion rate of magnesium in mantle minerals is usually higher than that of oxygen (Chakraborty et al. 1994; Xu et al. 2011). The activation energies for Mg–Fe interdiffusion in orthopyroxene and for Mg tracer diffusion in olivine have been determined to be 2.71 eV (Ganguly and Tazzoli 1994) and 2.85 eV (Chakraborty et al. 1994), respectively, which is comparable to that (2.46–2.99 eV) obtained by conductivity measurement in orthopyroxene at high-temperature region. Thus, the high ΔH obtained at high temperatures in this study would imply that the conduction in orthopyroxene is controlled not by oxygen vacancies, but by Mg vacancy (V''_{Mg}) as proposed by Schock et al. (1989) and Yoshino et al. (2009).

An ionic conduction mechanism is likely to have a positive activation volume of the order of an ionic volume, that is, in the range of several cm^3/mol (Keyes 1963). The activation volume calculated from the conductivity data obtained at high temperatures is 1.8–3.9 cm^3/mol by fitting Eq. (3). This value is in agreement with that derived from ab initio calculation for the formation of the Mg vacancy (4.43 cm^3/mol) in forsterite between 0 and 10 GPa (Béjina et al. 2009) and experimental measurements of the activation volume of Mg diffusion (1–7 cm^3/mol) in olivine (Chakraborty et al. 1994; Holzapfel et al. 2007). Therefore, the large positive activation volume also supports Mg vacancies as the dominant charge carriers in orthopyroxene at higher temperatures.

Formalism of the electrical conductivity of Fe-bearing orthopyroxene

A decrease in activation energy for Fe-bearing orthopyroxene with X_{Fe} can be approximated by the following equation for an *n*-type semiconductor at constant pressure (Debye and Conwell 1954; Yoshino and Katsura 2009):

$$\Delta E = \Delta E_0 - \alpha (X_{Fe})^{1/3} \quad (6)$$

where X_{Fe} is the mole fraction of iron in the Mg site, ΔE is the activation energy at a specific X_{Fe}, ΔE_0 is the activation energy at very low Fe concentrations, and α is a constant that accounts for a geometrical factor. A decrease in activation energy with total Fe content is associated with a decrease in the average Fe^{3+}–Fe^{2+} distance (Fig. 7). If both ionic conduction and small polaron are taken into account, the electrical conductivity of orthopyroxene can be expressed as (Yoshino 2010; Yoshino et al. 2012):

Table 2 Fitting parameters obtained from Eq. (7) for the electrical conductivity of orthopyroxene

σ_0^i (S/m)	ΔE_0^i (eV)	ΔV_0^i (cm^3/mol)	σ_0^h (S/m)	ΔE_0^h (eV)	α	ΔV_0^h (cm^3/mol)	β
855,610 (39)	2.51 (2)	4.15 (71)	163 (1)	2.33 (1)	1.99 (6)	1.06 (44)	0.12 (76)

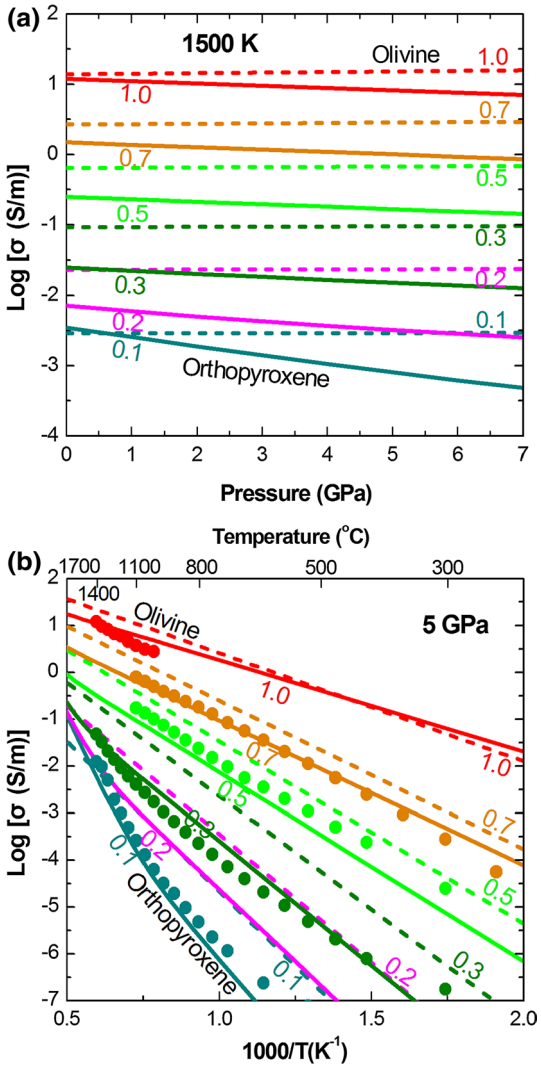

Fig. 9 Calculated electrical conductivity of orthopyroxene as a function of temperature, pressure and X_{Fe} based on the fitting parameters shown in Table 2. *Dashed* and *solid lines* indicate the calculated results of olivine and orthopyroxene, respectively. **a** Electrical conductivity for various Fe contents as a function of pressure at 1500 K. **b** Electrical conductivity of orthopyroxene at 5 GPa as a function of reciprocal temperature. Note that the *closed circles* represent the experimental data obtained in this study

$$\sigma = \sigma_0^i \exp\left[-\frac{(\Delta E_0^i + P\Delta V_0^i)}{k_B T}\right] + \sigma_0^p X_{Fe} \exp\left\{-\frac{\left[\Delta E_0^p - \alpha X_{Fe}^{1/3} + P(\Delta V_0^p - \beta X_{Fe})\right]}{k_B T}\right\} \quad (7)$$

where superscripts i and p represent ionic and small polaron conductions, respectively, and β is a constant. For the global least squares fitting, the fitting parameters for orthopyroxene are summarized in Table 2. The variations of conductivity values as a function of temperature, pressure and X_{Fe} determined from Eq. (7) can explain the present data (Fig. 9).

We now compare the present results obtained from fitting Eq. (7) with those of olivine as a function of temperature, pressure and X_{Fe} (Fig. 9). Although there are many studies on the conductivity of olivine (Hinze et al. 1981; Omura et al. 1989; Hirsch et al. 1993; Yoshino et al. 2012), our results can be directly compared to those of olivine aggregates of Yoshino et al. (2012) because of the similar experimental conditions adopted. As shown in Fig. 9a, at constant temperature, the electrical conductivity of orthopyroxene decreases with increasing pressure due to a positive activation volume as obtained in this study. However, this trend is opposite for olivine because the activation volume is negative for olivine. Consequently, the difference in conductivity between orthopyroxene and olivine becomes larger with increasing pressure. The parameters related to activation volume ($\Delta V_0^h, \beta$) imply that the value of activation volume in orthopyroxene is always positive within the stability field of orthopyroxene as compared to a small negative one in olivine. At higher temperatures corresponding to the upper mantle, the pressure dependence on the electrical conductivity of orthopyroxene becomes significantly larger with decreasing X_{Fe}, whereas that of olivine is very small (Fig. 9a). Such observations suggest that ionic conduction may become more important for orthopyroxene in the deep regions of the upper mantle. On the other hand, the pre-exponential factor (σ_0) of olivine obtained by Yoshino et al. (2012) is more than three times higher than that of orthopyroxene in this study, while the activation energy for olivine (1.96 eV: Yoshino et al. 2012) is smaller than that of orthopyroxene (2.33 eV: this study). Therefore, at the same pressure the electrical conductivity of olivine with low X_{Fe} ($\leq$0.3) is at least one order of magnitude higher than that of orthopyroxene (Fig. 9b) at low-temperature range. However, the difference in conductivity between olivine and orthopyroxene becomes smaller with increasing iron content.

Geophysical implications

The upper mantle is mainly composed of olivine (60 vol%). The present study demonstrates that the electrical

conductivity of Al-free orthopyroxene is lower than that of olivine. As shown in Fig. 9, unless orthopyroxene has unrealistically high Fe content ($X_{Fe} > 0.2$), the upper mantle conductivity should be controlled by olivine instead of orthopyroxene. On the other hand, orthopyroxene can contain a considerable amount of Al in mantle peridotite, especially below 3 GPa. Furthermore, Al-bearing orthopyroxene can store significant water in its crystal structure (Mierdel et al. 2007). The electrical conductivity of hydrous Al-bearing orthopyroxene significantly increases (Zhang et al. 2012). Below 3 GPa, orthopyroxene would contribute to the enhancement of electrical conductivity in the upper mantle.

Above 3 GPa, Al in orthopyroxene progressively dissolves into garnet with pressure, and the proportion of orthopyroxene decreases with depth. The large positive activation volume for ionic conduction in orthopyroxene with low Fe content ($X_{Fe} = 0.1$) also reduces the conductivity of orthopyroxene with increasing pressure. Although some studies suggested a negative pressure dependence of the electrical conductivity of olivine (Omura et al. 1989; Xu et al. 2000), the activation volume is much smaller than that of orthopyroxene. On the other hand, it has been widely accepted that the oxidation state of the shallow upper mantle is close to the QFM buffer but deeper upper mantle may be close to the IW buffer (Xu et al. 2000; Frost and McCammon 2008). Small polaron conduction is also controlled by $Fe^{3+}/\sum Fe$ in minerals, in other words, fO_2. For example, the electrical conductivity of olivine slightly increases with increasing fO_2 (Du Frane et al. 2005). Because the oxidation state of the upper mantle becomes more reduced with depth, the electrical conductivity of orthopyroxene is expected to be slightly lower than the present results. Therefore, orthopyroxene may have little effect on the electrical conductivity structure of the upper mantle above 3 GPa.

Concluding remarks

The electrical conductivity of orthopyroxene with various levels of iron content was measured as a function of pressure, temperature and total iron content in a Kawai-type multianvil apparatus. In all cases, the conductivity increased and the activation enthalpy decreased with increasing total Fe content. The present conductivity results reveal a positive activation volume, suggesting that the electrical conductivity decreased with increasing pressure at a constant temperature. The relationship between the logarithm of the electrical conductivity and the reciprocal temperature is consistent with Fe^{2+}–Fe^{3+} electron hopping (small polarons) as the dominant conduction mechanism at low temperatures (<1373 K) and ionic conduction via Mg vacancy mobility at higher temperatures (>1473 K). Since dry orthopyroxene with $X_{Fe} = 0.1$ relevant to the upper mantle has a lower conductivity than that of olivine, Al-free orthopyroxene may have little effect on the electrical conductivity structure of the upper mantle above 3 GPa.

Acknowledgements Two anonymous reviewers provided constructive comments and reviews that improved this paper. We would like to thank Fang Xu for XRD analysis, Shigeru Yamashita and Chengcheng Zhao for FT-IR measurements, and Daisuke Yamazaki, Akira Yoneda, Eiji Ito for their suggestions and discussions. This study was supported by the Strategic Priority Research Program (B) of the Chinese Academy of Sciences (XDB 18010401), the 1000Plan Program for Young Talents, Hundred Talent Program of CAS and NSF of China (41303048) to BZ, and also partially supported by the International Cooperative Research Program of Institute for Planetary Materials, Okayama University.

References

Akashi A, Nishihara Y, Takahashi E, Nakajima Y, Tange Y, Funakoshi K (2009) Orthoenstatite/clinoenstatite phase transformation in $MgSiO_3$ at high-pressure and high-temperature determined by in situ X-ray diffraction: implications for nature of the X discontinuity. J Geophys Res 114:B04206

Akimoto S, Katsura T, Syono Y, Fujisawa H, Komada E (1965) Polymorphic transition of pyroxenes $FeSiO_3$ and $CoSiO_3$ at high pressures and temperatures. J Geophys Res 70:5269–5278

Akimoto S, Komada E, Kushiro I (1967) Effect of pressure on the melting of olivine and spinel polymorph of Fe_2SiO_4. J Geophys Res 72:679–686

Béjina F, Blanchard M, Wright K, Price GD (2009) A computer simulation study of the effect of pressure on Mg diffusion in forsterite. Phys Earth Planet Inter 172:13–19

Chakraborty S, Faver JR, Yund RA, Rubie DC (1994) Mg tracer diffusion in synthetic forsterite and San Carlos olivine as a function of P, T and fO_2. Phys Chem Miner 21:489–500

Dai L, Karato S (2009) Electrical conductivity of orthopyroxene: implications for the water content of the asthenosphere. Proc Jpn Acad B 85:466–475

Dai LD, Li HP, Hu HY, Shan SM (2010) The electrical conductivity of dry polycrystalline olivine compacts at high temperatures and pressures. Mineral Mag 74:849–857

Debye PP, Conwell EM (1954) Electrical properties of N-type germanium. Phys Rev 93:693–706

Dobson DP (2003) Oxygen ionic conduction in $MgSiO_3$ perovskite. Phys Earth Planet Inter 139:55–64

Dobson DP, Brodholt JP (2000) The electrical conductivity of the lower mantle phase magnesiowüstite at high temperatures and pressures. J Geophys Res 105:531–538

Du Frane WL, Roberts JJ, Toffelmier DA, Tyburczy JA (2005) Anisotropy of electrical conductivity in dry olivine. Geophys Res Lett 32:L24315

Duba AG, Boland JN, Ringwood AE (1973) The electrical conductivity of pyroxene. J Geol 81:727–735

Frost DJ, McCammon C (2008) The redox state of Earth's mantle. Ann Rev Earth Planet Sci 61:1565–1574

Ganguly J, Tazzoli V (1994) Fe^{2+}–Mg interdiffusion in orthopyroxene: retrieval from the data on intracrystalline exchange reaction. Am Mineral 79:930–937

Goddat A, Peyronneau J, Poirier JP (1999) Dependence on pressure of conduction by hopping of small polarons in minerals mantle. Phys Chem Miner 27:81–87

Guo X, Yoshino T, Katayama I (2011) Electrical conductivity anisotropy of deformed talc rocks and serpentinites at 3GPa. Phys Earth Planet Inter 188:69–81

Hinze E, Will G, Cemic L (1981) Electrical conductivity measurements on synthetic olivines and on olivine, enstatite and diopside from Dreiser Weiher, Eifel (Germany) under defined thermodynamic activities as a function of temperature and pressure. Phys Earth Planet Inter 25:245–254

Hirsch LM, Shankland TJ, Duba AG (1993) Electrical conductivity and polaron mobility in Fe-bearing olivine. Geophys J Int 114:36–44

Holland TJB (1980) The reaction albite = jadeite + quartz determined experimentally in the range 600–1200 °C. Am Mineral 65:129–134

Holzapfel C, Chakraborty S, Rubie DC, Frost DJ (2007) Effect of pressure on Fe–Mg, Ni and Mn diffusion in $(Fe_xMg_{1-x})_2SiO_4$ olivine. Phys Earth Planet Inter 162:186–198

Huebner JS, Duba A, Wiggins LB (1979) Electrical conductivity of pyroxene which contains trivalent cations: laboratory measurements and the lunar temperature profile. J Geophys Res 84:4652–4656

Katsura T, Yokoshi S, Kawabe K, Shatskiy A, Okube M, Fukui H, Ito E, Nozawa A, Funakoshi K (2007) Pressure dependence of electrical conductivity of (Mg, Fe)SiO3 ilmenite. Phys Chem Miner 34:249–255

Keyes RW (1963) Continuum models of the effect of pressure on activated process. In: Paul W, Warschauer DM (eds) Solids under pressure. McGraw-Hill, New York, pp 71–99

Mierdel K, Keppler H, Smyth JR, Langenhorst F (2007) Water solubility in aluminous orthopyroxene and the origin of Earth's asthenosphere. Science 315:364–368

Nestola F, Ballaran TB, Balic-Zunic T, Secco L, Negro D (2008) The high-pressure behavior of an Al- and Fe-rich natural orthopyroxene. Am Mineral 93:644–652

Ohta K, Hirose K, Onoda S, Shimizu K (2007) The effect of iron spin transition on electrical conductivity of magnesiowüstite. Proc Jpn Acad Ser B 83:97–100

Omura K, Kurita K, Kumazawa M (1989) Experimental study of pressure dependence of electrical conductivity of olivine at high temperatures. Phys Earth Planet Inter 57:291–303

Paterson MS (1982) The determination of hydroxyl by infrared absorption in quartz, silicate glasses and similar materials. Bull Mineral 105:20–29

Poirier JP (1991) Introduction to the physics of the Earth's interior. Cambridge University Press, Cambridge, p 264

Ringwood AE (1975) Composition and petrology of the earth's mantle. McGraw-Hill, New York

Romano C, Poe BT, Kreidie N, McCammon CA (2006) Electrical conductivities of pyrope-almandine garnets up to 19 GPa and 1700 °C. Am Mineral 91:1371–1377

Schock RN, Duba AG, Shankland TJ (1989) Electrical conduction in olivine. J Geophys Res 94:5829–5839

Seifert KF, Will G, Voigt R (1982) Electrical conductivity measurements on synthetic pyroxenes $MgSiO_3$–$FeSiO_3$ at high pressures and temperatures under defined thermodynamic conditions. In: Schreyer W (ed) High-pressure researches in geoscience. Schweizerbart'sche, Stuttgart, pp 419–432

Shankland TJ, Peyronneau J, Poirier JP (1993) Electrical conductivity of the Earth's lower mantle. Nature 344:453–455

Sinmyo R, Pesce G, Greenberg E, McCammon C, Dubrovinsky L (2014) Lower mantle electrical conductivity based on measurements of Al, Fe-bearing perovskite under lower mantle conditions. Earth Planet Sci Lett 393:165–172

Xu Y, McCammon C (2002) Evidence for ionic conductivity in lower mantle (Mg, Fe)(Si, Al)O3 perovskite. J Geophys Res 107:2251

Xu Y, Shankland TJ (1999) Electrical conductivity of orthopyroxene and its high pressure phases. Geophys Res Lett 26:2645–2648

Xu Y, Shankland TJ, Duba AG (2000) Pressure effect on electrical conductivity of mantle olivine. Phys Earth Planet Inter 118:149–161

Xu JS, Yamazaki D, Katsura T, Wu XP, Remmert P, Yurimoto H, Chakraborty S (2011) Silicon and magnesium diffusion in a single crystal of $MgSiO_3$ perovskite. J Geophys Res 116:B12205

Yang X, Keppler H, McCammon C, Ni HW (2012) Electrical conductivity of orthopyroxene and plagioclase in the lower crust. Contrib Mineral Petrol 163:33–48

Yoshino T (2010) Laboratory electrical conductivity measurement of mantle minerals. Surv Geophys 31:163–206

Yoshino T, Katsura T (2009) Effect of iron content on electrical conductivity of ringwoodite, with implications for electrical structure in the mantle transition zone. Phys Earth Planet Inter 174:3–9

Yoshino T, Matsuzaki T, Yamashita S, Katsura T (2006) Hydrous olivine unable to account for conductivity anomaly at the top of the asthenosphere. Nature 443:973–976

Yoshino T, Matsuzaki T, Shatskiy A, Katsura T (2009) The effect of water on the electrical conductivity of olivine aggregates and its implications for the electrical structure of the upper mantle. Earth Planet Sci Lett 288:291–300

Yoshino T, Ito E, Katsura T, Yamazaki D, Shan S, Guo X, Nishi M, Higo Y, Funakoshi K (2011) Effect of iron content on electrical conductivity of ferro-periclase with implications for the spin transition pressure. J Geophys Res 116:B04202

Yoshino T, Shimojuku A, Shan S, Guo X, Yamazaki D, Ito E, Higo Y, Funakoshi K (2012) Effect of temperature, pressure and iron content on electrical conductivity of olivine and its high-pressure polymorphs. J Geophys Res 117:B08205

Yoshino T, Kamada S, Zhao C, Ohtani E, Hirao N (2016) Electrical conductivity model of Al-bearing bridgmanite with implications for the electrical structure of the Earth's lower mantle. Earth Planet Sci Lett 434:208–219

Zhang B, Yoshino T, Wu X, Matsuzaki T, Shan S, Katsura T (2012) Electrical conductivity of enstatite as a function of water content: implications for the electrical structure in the upper mantle. Earth Planet Sci Lett 357–358:11–20